Applied Energy 183 (2016) 1550–1564

Contents lists available at ScienceDirect

Applied Energy

journal homepage: www.elsevier.com/locate/apenergy

Investigation of reactions in a fluidized bed reactor during chemical looping combustion of coal/steam with copper oxide-iron oxide-alumina oxygen carrier

Ranjani Siriwardane [a,*], William Benincosa [a,b,c], Jarrett Riley [a,b], Hanjing Tian [a,b], George Richards [a]

[a] U.S. Department of Energy, National Energy Technology Laboratory, 3610 Collins Ferry Road, P.O. Box 880, Morgantown, WV 26507-0880, USA
[b] Department of Chemical Engineering, West Virginia University, Morgantown, WV 26505, USA
[c] Oak Ridge Institute for Science and Education, P.O. Box 117, Oak Ridge, TN 37831, USA

HIGHLIGHTS

- Fluidized bed reactor study of coal/CuO-Fe_2O_3-Aluminia (OC) is reported.
- TPR showed increased rates of gasification/combustion of coal in the presence of OC.
- Reduced OC promoted the water gas shift reaction in the presence of steam.
- Partially reduced OC promoted H_2 and CO_2 production in the presence of coal/steam.
- Increase in steam content negatively affected the chemical looping oxygen uncoupling.

ARTICLE INFO

Article history:
Received 1 June 2016
Received in revised form 30 August 2016
Accepted 17 September 2016

Keywords:
Chemical looping combustion of coal
Oxygen carrier
Coal gasification
Fluidized bed
Chemical looping combustion reactions
Coal volatiles

ABSTRACT

This paper presents data on conversion of two different coals with a chemical looping oxygen carrier, CuO-Fe_2O_3-alumina, and over a range of conditions including steam and various levels of reduction of the oxygen carrier.

Reactions of coal/steam/CuO-Fe_2O_3-alumina oxygen carrier and coal/steam/partially reduced CuO-Fe_2O_3-alumina oxygen carrier were investigated with Wyodak coal and Illinois #6 coal in a fluidized bed reactor. Temperature programmed reaction studies indicated that the oxygen carrier enhanced the steam gasification/combustion rates of both coals. Rates of gasification/combustion were higher with Wyodak coal (sub bituminous) than that with Illinois #6 coal (bituminous). In addition to the increase in reaction rates, the total moles of carbon that were gasified and combusted from coal/steam increased in the presence of the oxygen carrier. The reduced oxygen carrier promoted the water-gas shift reaction when reacted with synthesis gas in the presence of steam, but the reverse water gas shift reaction was observed when steam was not present. The partially reduced oxygen carrier enhanced the production of H_2 from coal/steam, which was different from the observations with un-reduced oxygen carrier. Water splitting reaction to produce H_2 was also observed with the reduced oxygen carrier. CuO-Fe_2O_3-alumina reacted with coal during the temperature ramp to 850 °C even in the absence of steam due to the chemical-looping oxygen uncoupling (CLOU) reaction. Fourier transform infra-red (FTIR) analysis indicated the presence of volatile aromatics during the temperature ramp and these may have also contributed to the reactions with the oxygen carrier in the absence of steam. Increasing steam concentration had a negative effect on the CLOU reaction.

Published by Elsevier Ltd.

1. Introduction

Chemical-looping combustion (CLC) is a novel combustion technology [1–8] that utilizes an oxygen carrier, such as metal oxide, to transport oxygen from the air to the fuel, thereby avoiding direct contact between fuel and air. The significant advantage of CLC over conventional combustion is that CLC can produce a storage-ready carbon dioxide (CO_2) stream—not diluted by nitrogen (N_2)—without expending any major energy required for the separation of CO_2. The overall CLC process, in which the metal oxide cycles between oxidized and reduced states, is exothermic.

* Corresponding author.
E-mail address: ranjani.siriwardane@netl.doe.gov (R. Siriwardane).

http://dx.doi.org/10.1016/j.apenergy.2016.09.045
0306-2619/Published by Elsevier Ltd.

The concept of CLC with solid fuels such as coal has been investigated extensively in the past [9–15], and progress of the CLC technology for solid fuel combustion has been presented in various review articles and books [16–21]. Recent research work in coal CLC include oxygen carrier development [22–27] and pilot-scale demonstrations [28–41].

Fluidized bed reactor tests have been conducted to understand the reaction performance of coal CLC with various oxygen carriers. Steam is generally used to promote the initial coal gasification reaction. It is usually assumed [17] that reactions proceed through indirect reduction with the aid of gaseous intermediates. It has also been reported that coal volatiles or synthesis gas produced by steam gasification of coal may initiate the reaction with metal oxides [13,17].

Other researchers [42–47] have proposed a mechanism known as the chemical-looping oxygen uncoupling (CLOU) process as a method to utilize oxygen from the metal oxide decomposition for combusting solid fuel. The CLOU process was designed at temperatures at which there is substantial equilibrium partial pressure of oxygen due to decomposition of the metal oxide. The CLOU process has been demonstrated experimentally at temperatures above 800 °C.

All of the above mentioned reaction mechanisms involve gas phase intermediates. We have shown that solid-solid reactions can occur with coal and oxygen carriers when there are significant contacts between the oxygen carrier and coal [48]. When CLC is conducted in a fluidized bed reactor, the contribution from the solid-solid interaction may not be significant.

Even though several reaction mechanisms for coal CLC in a fluidized bed reactor are reported, the proposed reaction mechanisms are speculative. In addition, the oxygen carrier is continuously reduced during the reaction with coal, and the effect of partially reduced oxygen carrier on the coal/steam reaction has not been reported.

The objective of the research work reported in this paper is to identify the various reactions that could occur when coal/steam are reacted with the oxygen carrier or the partially reduced oxygen carrier in a fluidized bed reactor. The results here aim at determining which reactions are important to consider, noting that steam, the coal type, the carrier type and the extent of carrier reduction are all contributing factors. The oxygen carrier selected in this study was CuO-Fe_2O_3-alumina, which has shown promising results with both methane and coal in our previous studies [49–53]. A large batch (180 kg) of the oxygen carrier was produced for demonstration testing in a 50-kWth chemical looping experiment, and some promising results from the pilot-scale test have been obtained. The reaction profiles of Illinois #6 coal or Wyodak coal with and without CuO-Fe_2O_3-alumina oxygen carrier over a range of conditions including steam and various levels of oxygen reduction are reported in the current study.

2. Experimental

2.1. Oxygen carriers

CuO-Fe_2O_3-alumina oxygen carriers [52] were prepared using the commercial spray drying method at Nextech Inc. The composition of the oxygen carrier was 30 wt.% CuO, 30 wt.% Fe_2O_3, and 40 wt.% alumina, and the particle size range was 74–250 μm. The material properties of the oxygen carrier are listed in Table 1.

2.2. Coal characterization

The compositions of the two coals, Wyodak and Illinois #6, are listed in Table 2. Illinois 6 coal, which is a bituminous coal has the highest carbon value and lowest volatile matter. Wyodak coal is a subbituminous coal and has higher volatile matter.

Table 1
Physical properties of copper ferrite oxygen carrier.

Particle sphericity	0.79–0.94
Particle density	3.13 g/cm^3
Bulk density (Fluffed)	1.32 g/cm^3
Void fraction (Fluffed)	0.58
Bulk density (Packed)	0.24 g/cm^3
Void fraction	0.53
Density measured by He Pycnometer	4.66 g/cm^3
Tapped density	1.45 g/cm^3
Particle size	74–250 μm

2.3. Temperature programmed reaction studies with coal in fluidized bed reactor tests

Minimum fluidization velocities (MFV) of CuO-Fe_2O_3-alumina oxygen carriers at various temperatures are listed in Table 3. The temperature programmed reaction (TPR) studies were carried out using a fluidized bed reactor manufactured by Autoclave Engineers HR-160 Reactor Assembly (Model # 5010-2377/HR-160). The oxygen carrier/coal bed height was 7.62 cm, and the diameter was 6 cm. The reactor column was made from Inconel SB-564 to withstand temperatures up to 900 °C. A ceramic porous plate with 15–40 μm pores was used as the gas distributor. The setup is equipped with three electrical heaters installed around the reactor to heat the reactor to the target temperature of 850 °C. Prior to the tests, 10 g each of coal and 322 g CuO-Fe_2O_3-alumina oxygen carriers were mixed. Then the mixture was heated from 25 °C to 850 °C at a heating rate of 4 °C/min in helium at a flow rate of 7.8 SLPM (24 × MFV of Fe-Cu/alumina at 850 °C). Then the sample was maintained at 850 °C for 0.5 h in helium. During the experiments, 30 vol.% steam was introduced either during the temperature ramp beginning at 300 °C or after the isothermal dwell at 850 °C. After the reducing reaction with coal, the sample was cooled to 750 °C to initiate oxidation with air for 1.5 h. The reactor effluent was monitored using a Pfeiffer Omnistar mass spectrometer. All the experiments were repeated and reproducibility has been excellent.

2.4. Diffuse reflectance Fourier transform infrared spectroscopy

Prior to use, the as-received coal samples were ground into a powder to maximize spectral quality via diffuse reflectance infrared Fourier transform spectroscopy (DRIFTS) analysis. For each test, a coal sample of approximately 20 mg was charged to a DRIFTS reactor cell (Thermo Electron product 0031-902). The DRIFTS cell is a cold-walled reactor that features temperature control and ZnSe windows for IR transmission within the 650–4000 cm^{-1} range. Helium was introduced to the coal sample to remove all the gases from the cell. Then the Helium flow was stopped and sample was heated from ambient to 800 °C. Infrared spectra were collected at various temperatures with a Thermo-Nicolet Nexus 670 FTIR instrument, which housed the DRIFTS reactor cell. Spectra were collected at a resolution of 4 cm^{-1} with 50 co-added scans using a liquid N_2-cooled MCT/A detector.

3. Results and discussion

When coal is reacted with an oxygen carrier in the presence of steam, various reactions can take place and some possible reactions are listed below.

- Coal gasification and subsequent gas reactions with oxygen carrier:

Table 2
Properties of coals.

Coal type	Particle size	Class	Ash (dry)	S (dry)	C (dmmf)	H (dmmf)	V.M. (dmmf)	kJ/kg (dmmf)
Wyodak	74–300 μm	hvCb	16.2	4.52	81.8	5.7	43.8	33,857
Illinois #6	74–300 μm	subB	7.6	0.43	76.2	6.2	48.1	30,789

Table 3
Minimum fluidization velocity of the copper ferrite oxygen carrier with temperature dependence.

Temperature (°C)	Minimum fluidization velocity (SLPM)
25	3.16
624	0.8
750	0.63
800	0.4
900	0.25

$$C + H_2O \rightarrow CO + H_2 \quad \Delta H_{800} = 135.74\ \frac{kJ}{mol} \tag{1}$$

$$H_2 + \textit{Metal Oxide} \rightarrow \textit{Reduced Metal Oxide} + H_2O \tag{2}$$

$$CO + \textit{Metal Oxide} \rightarrow \textit{Reduced Metal Oxide} + CO_2 \tag{3}$$

$$C + CO_2 \rightarrow 2CO \quad \Delta H_{800} = 169.44\ \frac{kJ}{mol} \tag{4}$$

- Chemical looping oxygen un-coupling (CLOU) mechanism:

$$4CuO \rightarrow 2Cu_2O + O_2 \quad \Delta H_{800} = 67.8\ \frac{kJ}{mol} \tag{5}$$

$$C + O_2 \rightarrow CO_2 \quad \Delta H_{800} = -395\ \frac{kJ}{mol} \tag{6}$$

- Solid-solid interaction:

$$MeO + C \rightarrow Me + CO_2 \tag{7}$$

- Water-gas shift (WGS) reaction catalyzed by reduced oxygen carrier:

$$CO + H_2O \rightarrow CO_2 + H_2 \quad \Delta H_{800} = -33.07\ \frac{kJ}{mol} \tag{8}$$

- Reduced oxygen carrier oxidation by steam:

$$2FeO + H_2O \rightarrow Fe_2O_3 + H_2 \quad \Delta H_{800} = -31.9\ \frac{kJ}{mol} \tag{9}$$

3.1. Steam gasification of coal without an oxygen carrier with steam at 300–850 °C

In order to understand the coal gasification process with steam, as shown in reaction (1), 30% steam was introduced during the temperature ramp of coal without the oxygen carrier. Fig. 1 shows the effluent gas concentrations during the temperature ramp of the two coals with steam and a comparative plot of cumulative moles of each gas produced. The comparative plot also displays the CO_2 produced during the oxidation segment of the experiments (PO CO_2) which was also included in the cumulative carbon balances. The steam gasification process appears to initiate around 600 °C with concentration peaks around 850 °C with both coals. The rate of steam gasification was significantly higher with Wyodak coal than that with Illinois #6 coal as indicated by the CO and H_2 peak maxima in Fig. 1. The H_2, CO and CO_2 peaks for Illinois #6 coal were very broad, slow continuous gas production was observed when the temperature was maintained at 850 °C, which was different from Wyodak coal. Wyodak coal, which is a sub-bituminous coal had a higher rate of production of synthesis gas with steam than Illinois #6 coal, which is a high rank coal as also shown in Fig. 1. It has been reported [55–58] that the properties of the char can affect the combustion performance. The char produced by Illinois #6 coal may have different properties than that produced by Wyodak coal and may have contributed to the different reaction rates and product distributions. Char porosity and surface area have shown to play an important role on the gasification reaction [57,58], and differences in char type affected the gasification rates as seen in Fig. 1. It was reported that [57,58] Wyodak coal has thermoset type char while Illinois #6 has thermoplastic type. The plastic coals like Illinois #6 are known to form chars with highly cellular pore structure, while non-plastic coals do not undergo drastic macro pore structural changes during the pyrolysis stage. Scanning electron micrographs of Wyodak coal char and Illinois #6 coal char are reported in Fig. 2 and it is clear that the surface morphologies of the two chars are different. Char from Illinois #6 coal had a smoother surface with some voids while the char from Wyodak coal appeared to have a rough surface. These differences in the surface morphology may also have contributed to the different char gasification rates. Even though the gasification rates were different, the cumulative moles of gases produced during gasification were very similar with the two coals, as shown in Fig. 1. Total moles of carbon from steam gasification followed by oxidation for Wyodak and Illinois #6 coals were 0.3 and 0.4, respectively. Illinois #6 has a higher carbon value than Wyodak coal, thus the data is consistent. In addition to the gasification products, the data indicated that the type of coal plays a major role in the steam gasification rates as well.

3.2. Effect of CuO-Fe_2O_3-alumina oxygen carrier on coal/steam (300–850 °C) interactions

Fig. 3 shows effluent gas compositions when coal and CuO-Fe_2O_3-alumina was heated in the presence of 30 vol.% steam from 300 to 850 °C and cumulative moles of gas produced. Repeated experiments characterizing the interaction between three components, coal, steam, and oxygen carrier, showed excellent reproducibility as also demonstrated in Fig. 3. In the experiments containing Wyodak coal, steam, and oxygen carrier, repeated runs reproduced the carbon dioxide peak concentrations by a difference of 0.4%, the total carbon molar production by 1.2%, and the full width half maximum of the major carbon dioxide peak concentrations by 3.2% and 3.3%. For the interaction between Illinois #6, steam, and oxygen carrier, repeated experiments reproduced the carbon dioxide peak concentrations by a difference of 4.5%, the total carbon molar production by 2.8% and the full width half maximum of the major CO_2 concentration peak by 2.8% and 11.0%. It should be noted that all results reported in this paper were verified by repeating the experiments, and all results were reproducible as such.

The concentration peak of CO_2 was significantly higher than the concentration peaks of H_2 and CO, with both coals indicating the faster reaction of synthesis gas derived from coal with the oxygen carriers to produce CO_2. The concentration peak of CO_2 with Wyodak coal was higher than that with Illinois #6 coal, indicating faster reaction rate with Wyodak coal. The reaction with Wyodak coal also takes place at a lower temperature than that with Illinois #6 coal which also indicated better reactivity of Wyodak coal. Cumulative moles of gases produced during the temperature ramp, also

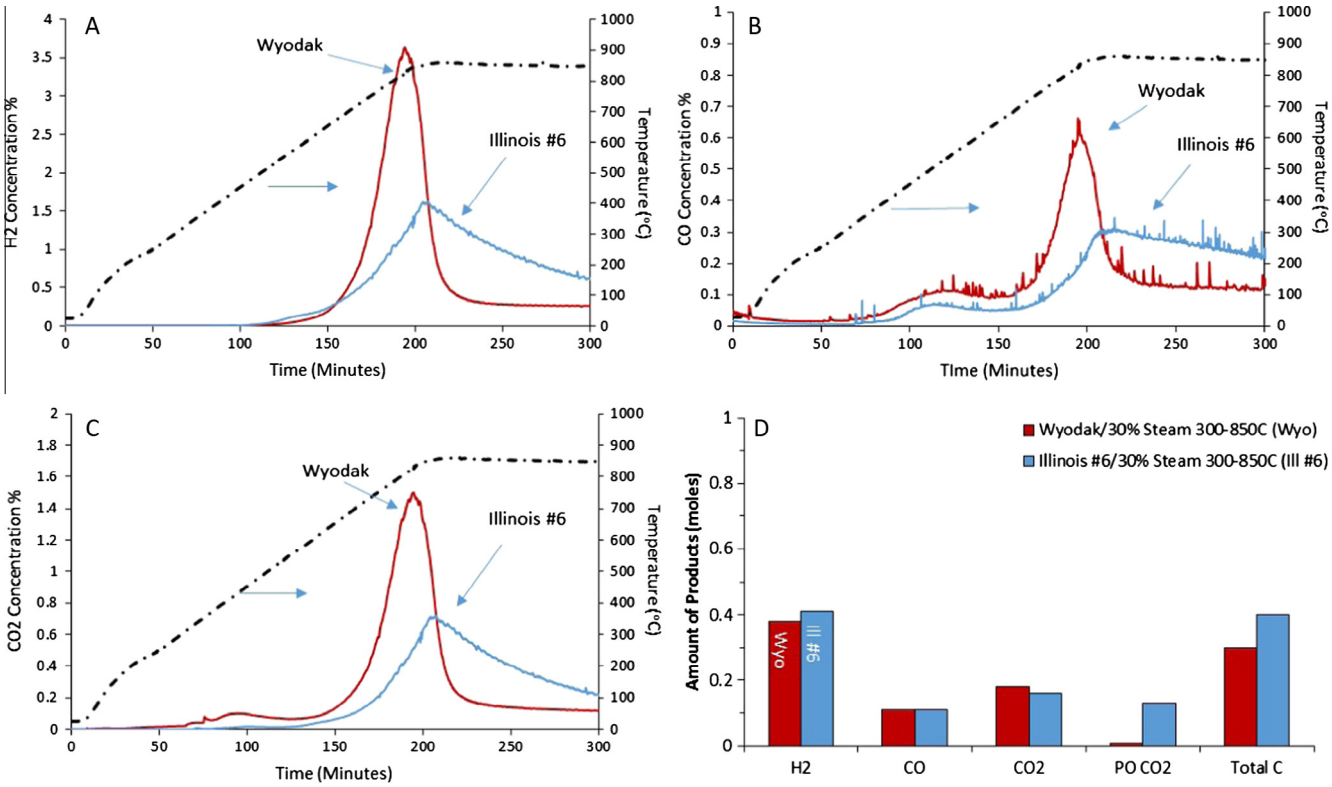

Fig. 1. Product gas composition during the temperature ramp (RT-850 °C) of Wyodak and Illinois #6 coal in the presence of steam (300–850 °C), without an oxygen carrier (A) H_2, (B) CO, (C) CO_2, (D) total molar production of gases.

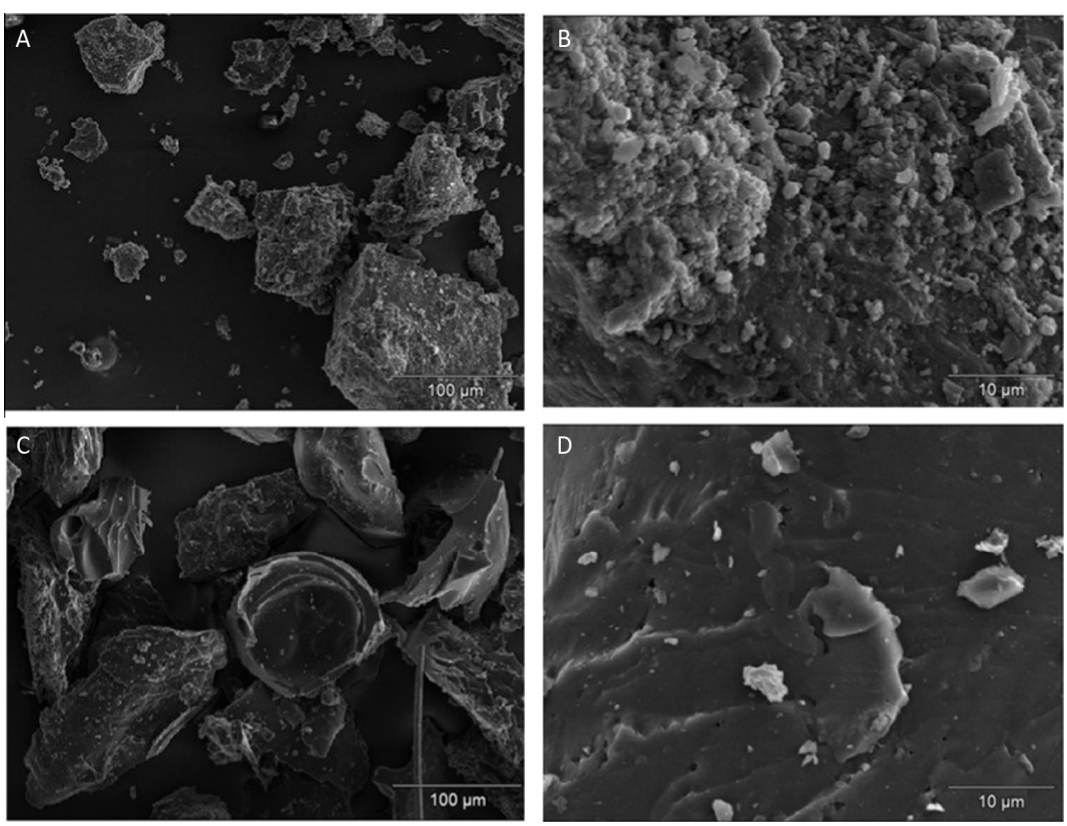

Fig. 2. Scanning electron micrographs of Wyodak (A, B) and Illinois #6 (C, D) coal chars at two different magnifications.

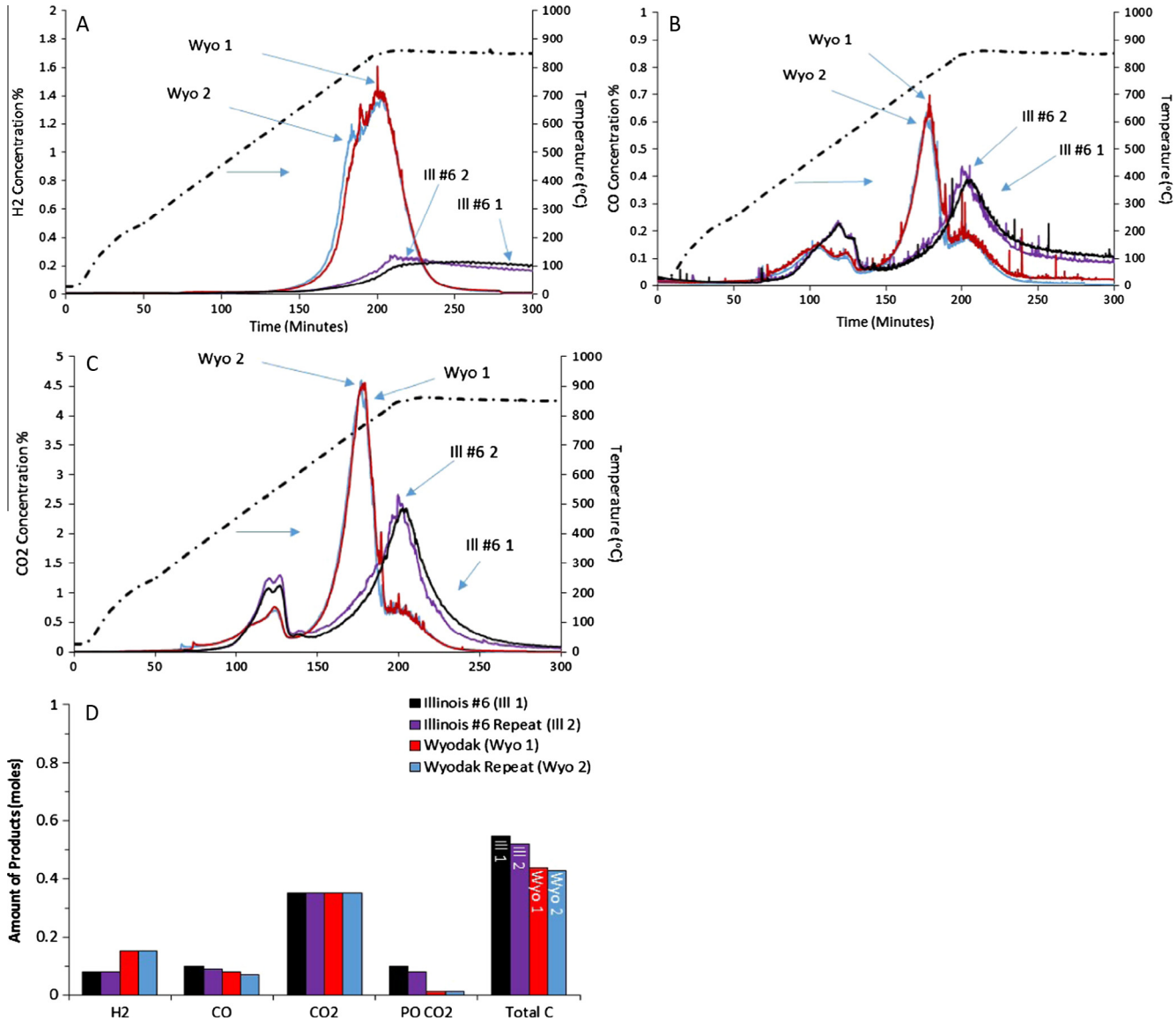

Fig. 3. Reproducibility of product gas composition during the temperature ramp (RT-850 °C) of Wyodak or Illinois #6 coal in the presence of steam (300–850 °C) and copper ferrite oxygen carrier (A) H_2, (B) CO, (C) CO_2, (D) total molar production of gases.

shown in Fig. 3, indicated that the amount of CO_2 produced as well as the total carbon gases (CO and CO_2) formed were similar with Illinois #6 coal and Wyodak coal. Thus, the total carbon combusted with both coals by the oxygen carrier were similar even though the rates of gasification and combustion were lower with Illinois #6 coal.

Comparative data on outlet gas concentrations during the temperature ramps in the presence of steam at 300–850 °C with Wyodak coal/steam/CuO-Fe_2O_3-alumina, and Wyodak coal/steam (blank) are shown in Fig. 4. The CO_2 peak concentration was higher, and the peak temperature was lower when the oxygen carrier was present with coal/steam, which indicated that rate production of CO_2 was faster when the oxygen carrier is present. The amount of H_2 produced from steam gasification of coal was significantly higher with blank Wyodak coal than that with coal/oxygen carrier due to the consumption of H_2 by the oxygen carrier. During the temperature ramp of Wyodak coal/steam/CuO-Fe_2O_3-alumina, the decrease in peak intensity of H_2 was more significant than that with CO indicating the faster consumption of H_2 from coal gasification by the oxygen carrier.

The cumulative gas products formed are also shown in Fig. 4. The total amount of CO and CO_2 produced with coal/steam/CuO-Fe_2O_3-alumina was higher than that with coal/steam, indicating that there was additional carbon oxide formation due to the presence the oxygen carrier. Since H_2O formed was not measured during the reaction, it was not possible to obtain an accurate measurement of the amount of oxygen utilized from the oxygen carrier for the reaction with hydrogen. A rough estimate was made using the cumulative data in Fig. 3: The quantity of hydrogen produced during coal/steam gasification was 0.38 mol and it decreased to 0.15 mol with coal/steam/oxygen carrier due to the consumption of H_2 by the oxygen carrier. The consumption of H_2 by the oxygen carrier was about 0.23 mol, assuming that there was no additional H_2 formed when the oxygen carrier was present with coal/steam and the consumption of CO was about 0.03 mol and the increase in CO_2 was 0.18 mol. The increase in the CO_2 does not correlate well with the decrease in CO, indicating that there was additional CO_2 formed by the increase in gasification/combustion due to the presence of the oxygen carrier. Thus, the presence of the oxygen carrier not only improves the gasification rate, but

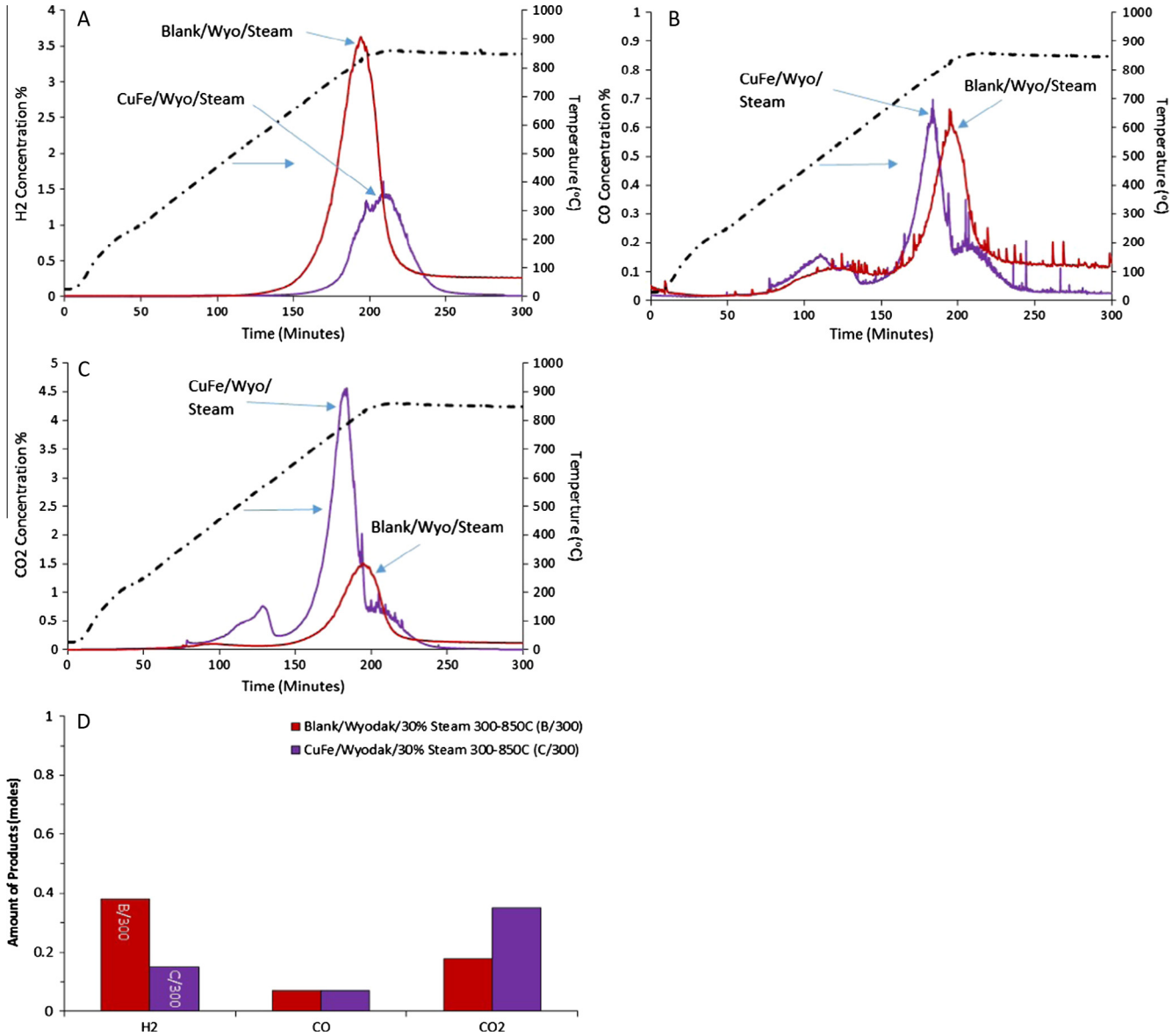

Fig. 4. Product gas composition during the temperature ramp (RT-850 °C) of Wyodak coal in the presence of steam (300–850 °C) or the copper ferrite oxygen carrier (A) H_2, (B) CO, (C) CO_2, (D) total molar production of gases.

it also increases the total carbon gasified. Saucedo et al. [25] reported that the presence of Fe_2O_3 led to an increase in the rate of gasification because of the rapid oxidation of CO by the oxygen carrier to CO_2 within the mass transfer boundary layer surrounding the char particle. This effect was most prominent when the surface area of the char was at its maximum due to the accompanying increase in porosity and pore size during the char gasification. Other researchers [26,54] have also observed an increase in coal gasification rates in the presence of oxygen carriers.

Comparative data on outlet gas concentrations during the temperature ramps (steam 300–850 °C) with Illinois #6 coal/steam/CuO-Fe_2O_3-alumina, and Illinois #6 coal/steam (blank) are shown in Fig. 5. When the oxygen carrier was present H_2 was consumed at a faster rate, CO was produced at an increased rate and there was a rapid increase in the CO_2 production rate. The total carbon oxides produced was higher when the oxygen carrier was present than that without the oxygen carrier, as also shown in Fig. 4, indicating that there was more carbon gasification/combustion (0.18 mol) when the oxygen carrier was present. The H_2 decreased about 0.33 mol, CO_2 increased about 0.19 mol, while the change in CO was insignificant (−0.01). Similar to the data above with Illinois #6 coal, CuO-Fe_2O_3 oxygen carrier promoted additional coal gasification/combustion with Wyodak coal as well.

3.3. Effect of steam on the interaction of synthesis gas derived from steam gasification of coal with CuO-Fe_2O_3-alumina oxygen carrier

When the synthesis gas derived from steam gasification (reactions (2) and (3)) of coal reacts with the oxygen carrier, the reaction performance may be affected by the presence of steam. In order to understand this effect, synthesis gas was reacted with the oxygen carrier in the presence of various concentrations of steam. Simulated synthesis gas composition was H_2: 7.6% (36.8 mmol/min), CO_2: 1.88% (9.1 mmol/min), CO: 1.58% (7.7 mmol/min) in helium. Steam concentrations of 0, 15 and 30% were introduced to the synthesis gas during the temperature ramps with the oxygen carrier, and effluent gas compositions were measured.

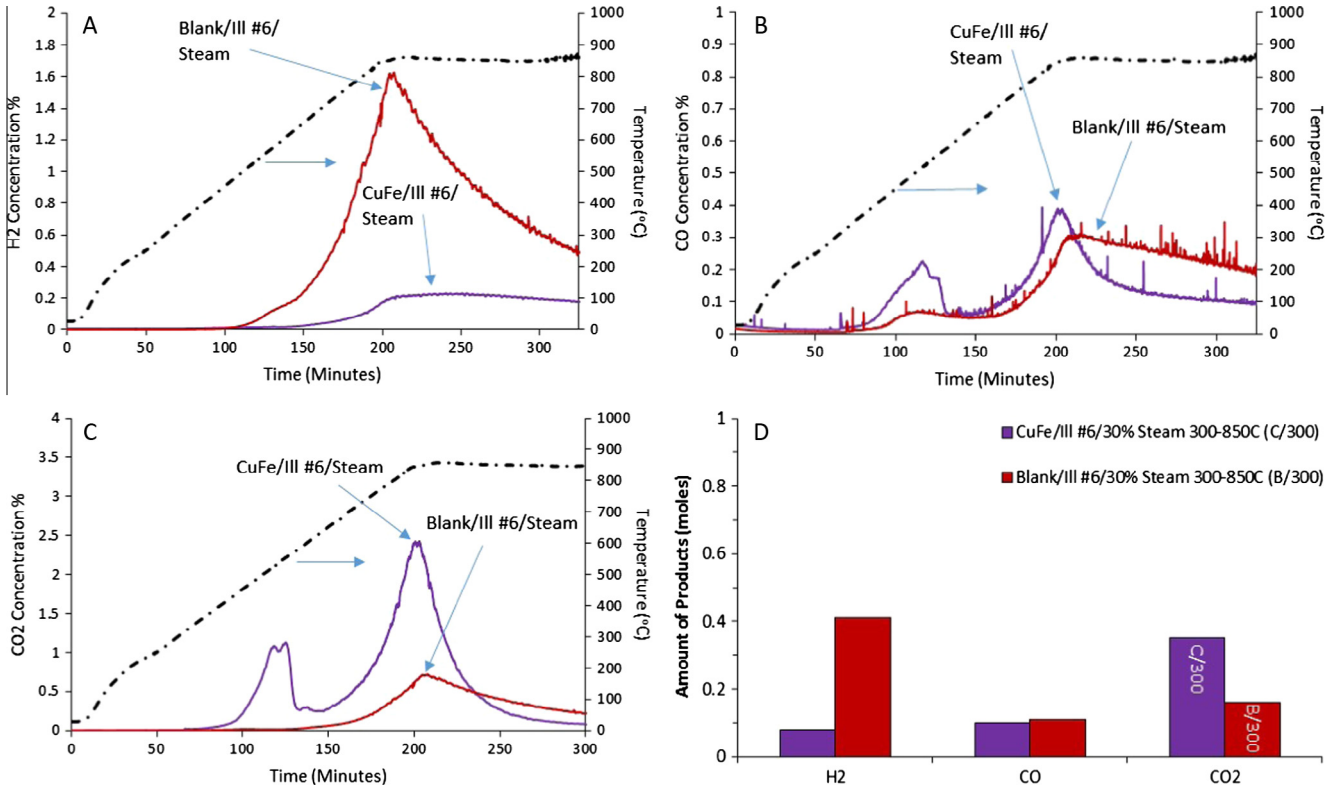

Fig. 5. Product gas composition during the temperature ramp (RT-850 °C) of Illinois #6 coal in the presence of steam (300–850 °C) or the copper ferrite oxygen carrier (A) H_2, (B) CO, (C) CO_2, (D) total molar production of gases.

The outlet gas compositions during the reaction of synthesis gas and CuO-Fe_2O_3-alumina oxygen carrier are shown in Fig. 6. The data indicated that CO and H_2 were consumed and CO_2 was generated during the temperature ramp due to the reaction of synthesis gas with the oxygen carrier. Steam has a significant effect on the reaction. After the initial reduction of the oxygen carrier, the effluent concentrations of the gases were strongly affected by the concentration of steam. When steam was present, CO concentration was lower than the initial concentration while H_2 and CO_2 were higher. The data indicated that the water-gas shift reaction (8) was catalyzed by the reduced oxygen carrier when steam was present to consume CO to produce CO_2 and H_2. Since steam is also consumed by the coal to produce synthesis gas, it is difficult to estimate the extent of the water-gas shift reaction by the reduced oxygen carrier in the coal/steam/oxygen carrier system since steam is also consumed for the coal gasification reaction.

It was also interesting to note that when steam was not present, after the initial reaction with oxygen carrier the CO concentration was higher than the initial concentration while the H_2 and CO_2 were lower. It appears that the reduced oxygen carrier was promoting the reverse water gas shift reaction (10) when steam was not present.

$$CO_2 + H_2 \rightarrow CO + H_2O \tag{10}$$

The increase in CO when steam was not present could also be due to the reaction of CO_2 with the reduced oxygen carrier (M) to form CO as shown in reaction (11)

$$Me + CO_2 \rightarrow CO + MeO \tag{11}$$

In order to understand this reaction, the oxygen carrier was reduced first with synthesis gas (CO_2 2.02%, CO 6.41%, H2 10.24%, and He 81.22), and then 28% CO_2 in helium was introduced at 800 °C. Formation of CO (results not shown) was not observed indicating that the reverse water-gas shift reaction (10) is the most possible explanation for the formation of additional CO when steam was not present. Repeated experiments showed similar results.

3.4. Interaction of coal/steam with reduced CuO-Fe_2O_3-alumina oxygen carrier

During the reaction of the oxygen carrier with coal/steam, the oxygen carrier is continuously reduced. The reduced carrier may have an effect on the initial coal gasification reaction with steam (reaction (1)). In order to understand how the reduced carrier affects the reaction, the CuO-Fe_2O_3-alumina oxygen carrier was reduced to various reduction states with methane and then the reduced oxygen carrier was mixed with coal, and temperature ramp was performed in the presence of steam.

Oxygen transfer capacities were calculated using equation (12). Experimental oxygen transfer capacity is based on the effluent gaseous products and the theoretical oxygen transfer capacity is based on the corresponding chemical reaction.

$$\textit{Oxygen Transfer Capacity} = \frac{[\text{Mol } CO_2 * 2\text{Mol O} + \text{Mol } H_2O * 1\text{Mol O}] * \frac{16.0\,\text{g}}{\text{mol}}}{\textit{Mass Oxygen Carrier}} \tag{12}$$

The reduced states of the oxygen carrier estimated from the percentage of oxygen transfer during the reaction with methane are listed in Table 4. The gas compositions during the temperature ramp with Wyodak coal/reduced oxygen carrier/steam and comparative data with the unreduced oxygen carrier are shown in Fig. 7. The CO_2 concentration peak was highest and both CO and H_2 concentration peaks were lowest with the unreduced oxygen carrier, indicating the highest rate of combustion because more oxygen atoms are available for the reaction with coal or synthesis gas. With increased reduction of the oxygen carrier, the rate of CO_2

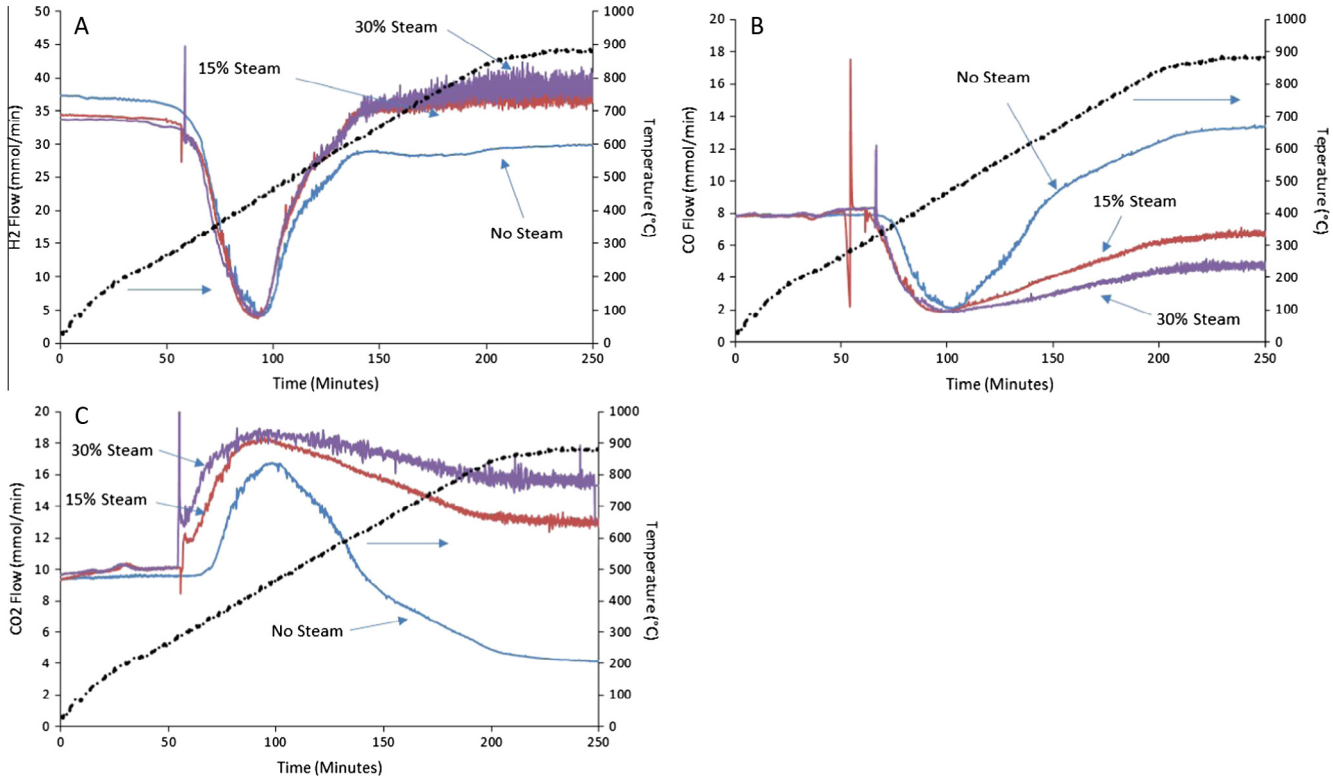

Fig. 6. Product gas flow rate during the temperature ramp (RT-850 °C) of the copper ferrite oxygen carrier in the presence of a simulated Illinois #6 synthesis gas and varying compositions of steam (300–850 °C) (A) H_2, (B) CO, (C) CO_2.

Table 4
Reduction states of copper and iron at various reduction times.

Reduction time	Experimental oxygen transfer capacity	Reduction reaction	Theoretical oxygen transfer capacity
5.5 min	5.5%	$4CuO + CH_4 \rightarrow 4Cu + CO_2 + 2H_2O$	6.0%
7 min	7.0%	$3CuO + 3Fe_2O_3 + CH_4 \rightarrow 3Cu + 2Fe_3O_4 + CO_2 + 2H_2O$	7.0%
12 min	8.0%	$3CuO + Fe_2O_3 + CH_4 \rightarrow 3Cu + 2FeO + CO2 + 2H_2O$	9.0%

production decreased and rate of CO and H_2 production increased since less oxygen atoms are available for the reaction with synthesis gas. Repeated experiments showed similar results.

The cumulative moles of gases produced are also shown in Fig. 7. It is interesting to note that amount of H_2 continuously increased with increased reduction of the oxygen carrier while there was no significant changes in the amounts of CO and CO_2. The cumulative carbon oxides ($CO + CO_2$) produced were similar with the reduced and un-reduced oxygen carriers. Even after reduction there were oxygens still available from the oxygen carrier for the reactions. However, it appears that total production of CO to CO_2 was not greatly affected by the oxygen carrier reduction, but the production of H_2 was affected.

A comparison of the effluent gas compositions of coal/steam without the oxygen carrier, with the unreduced oxygen carrier, and reduced oxygen carrier (12 min) are shown in Fig. 8. It is interesting to note that both CO and H_2 concentration peaks were highest with the reduced carrier/coal/steam than that with coal/steam without an oxygen carrier. It should also be noted that the concentration peaks of both CO and H_2 with reduced carrier/coal/steam were shifted to a lower temperature than that with coal/steam without the oxygen carrier. The data indicated that the reduced oxygen carrier was either promoting the coal gasification reaction rate or changing the reaction pathway. It has been reported that coal gasification reaction can be promoted by reduced iron oxide, but it is not clear how the reduced oxygen carrier promotes the gasification reaction in the fluidized bed reactor. Alkali incorporated Fe_2O_3 also has shown improved gasification of coal [22] in a fluid bed reactor but the reason for the improvement is not known. The cumulative product gas yields are also shown in Fig. 8. It is clear that the H_2 yield was higher with the reduced oxygen carrier/coal/steam than that with coal/steam, indicating that in addition to improving reaction rates, total moles of H_2 were also higher with the reduced oxygen carrier/coal/steam. Total CO produced with the reduced oxygen carrier/coal/steam was similar to that with coal/steam but the amount of CO_2 formed was higher with the reduced oxygen carrier. However, the increase in H_2 (0.33 mol) was higher than the increase in CO_2 (0.13 mol).

If the water-gas shift reaction is promoted by the reduced oxygen carrier there should be a corresponding increase in CO_2 similar to the H_2 increase and a decrease in the amount of CO. A small increase in CO_2 was observed with oxygen carrier/coal/steam as compared to that with coal/steam, but the change in the amount of CO was insignificant, indicating that the increase in H_2 with reduced oxygen carrier/coal/steam cannot be explained by the water-gas shift reaction. Since steam is consumed for the coal gasification reaction, the remaining steam concentration in the gas stream may not be adequate for promoting the water-gas shift reaction.

It is possible that in addition to the reaction (1), H_2 formation facilitated by the water splitting reaction (9) may also be occurring in the presence of reduced oxygen carrier.

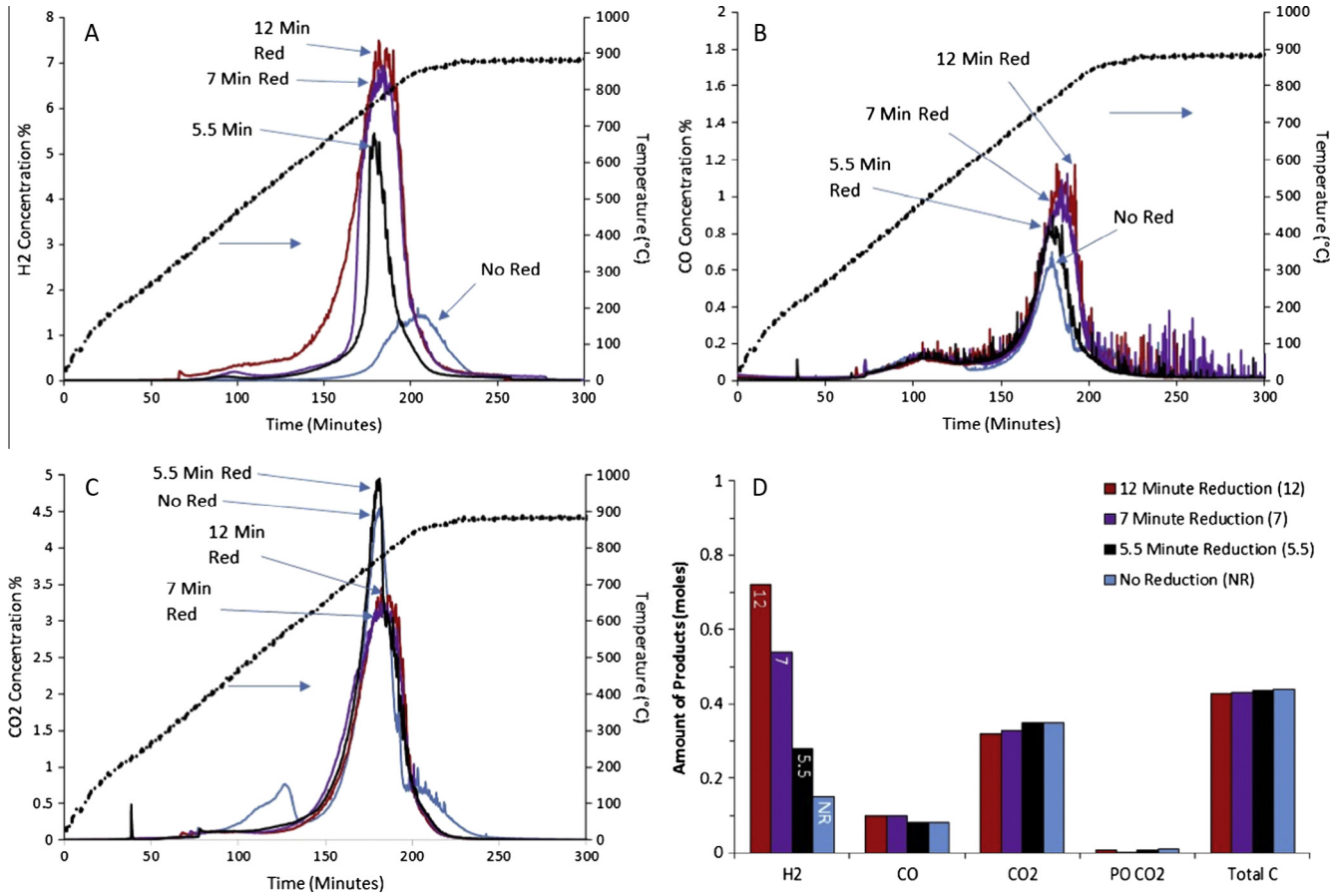

Fig. 7. Product gas composition during the temperature ramp (RT-850 °C) of reduced and unreduced copper ferrite oxygen carrier in the presence of 30% steam (300–850 °C) and Wyodak coal (A) H_2, (B) CO, (C) CO_2, (D) total molar production of gases.

3.5. Interaction of reduced CuO-Fe_2O_3-alumina carrier with steam

In order to understand the H_2O splitting reaction by the reduced oxygen carrier to produce H_2 by reaction (9), the oxygen carrier was first reduced with methane for 5.5 min., 7 min. and 12 min. to obtain different oxidation states, and then a temperature ramp was conducted in the presence of 30% steam without coal.

As shown in Fig. 9, H_2 concentration increased with increasing reduction of the oxygen carrier but the H_2 concentration was below 0.12 vol.%. Repeated experiments show similar results. The increase in H_2 production rate and total moles with the reduced oxygen carrier/coal/steam in Fig. 8, cannot be fully explained by this water splitting reaction since the contribution is low. The reaction of steam with the reduced Fe^0/Fe^{+2} is favorable [19], while it is not favorable with Cu^0. Thus, the contribution may be only due to the iron component in the oxygen carrier. However, this reaction may be enhanced when the coal is present due to the consumption of oxygen by carbon to form CO_2.

3.6. Effect of addition of steam at 850 °C on the reaction of CuO-Fe_2O_3-alumina with coal

In order to understand the effect of steam addition temperature, Wyodak coal/CuO-Fe_2O_3-alumina was heated to 850 °C without steam and 30% steam was added at 850 °C. The results are shown in Fig. 10. For comparison, the data with Wyodak coal/CuO-Fe_2O_3-alumina/steam addition at 300 °C and a blank data of Wyodak coal/steam addition at 850 °C without the oxygen carrier are also shown in Fig. 10. During the initial temperature ramp of coal without steam to 850 °C, only minute amounts of H_2, CO, and CO_2 were observed but high concentration peaks of H_2, CO, and CO_2 were observed when steam was introduced at 850 °C. The H_2, CO, and CO_2 concentration peaks when steam was introduced at 850 °C to coal were higher than that when steam was introduced at 350–800 °C (Fig. 1), indicating fast gasification rates at 850 °C as expected.

The product gases when Wyodak coal/CuO-Fe_2O_3-alumina was heated in the absence of steam up to 850 °C and during steam addition at 850 °C are also shown in Fig. 10. It is interesting to note that the CO_2 concentration peak was high during the temperature ramp even in the absence of steam. This is possibly due to coal directly reacting with the oxygen released from the CuO via CLOU reactions (5) and (6). The CO_2 peak solely due to the reaction of coal with oxygen from CLOU reaction was at a higher temperature than that with Wyodak coal/CuO-Fe_2O_3-alumina/steam 300–850 °C, indicating that synthesis gas from coal steam gasification react with the oxygen carrier at a lower temperature than the CLOU oxygen/coal reaction temperature. There was also a CO peak during the temperature ramp without steam. The concentration peaks of both CO_2 and CO for Wyodak coal/CuO-Fe_2O_3-alumina/steam at 850 °C, were lower than that with Wyodak coal/CuO-Fe_2O_3-alumina/steam at 300–850 °C because some coal has already reacted with the oxygen released from the oxygen carrier via CLOU reaction prior to the introduction of steam at 850 °C. The best CO_2 production rate and the highest CO_2 amounts were observed when steam was introduced at 300 °C during the temperature ramp due to the combination of CLOU and gasification/combustion/CLOU reactions occurring simultaneously at 700–800 °C.

Comparative data on outlet gas concentrations during the temperature ramps with Illinois #6 coal/steam at 300–850 °C/CuO-Fe_2O_3-alumina, Illinois #6 coal/steam at 850 °C base line,

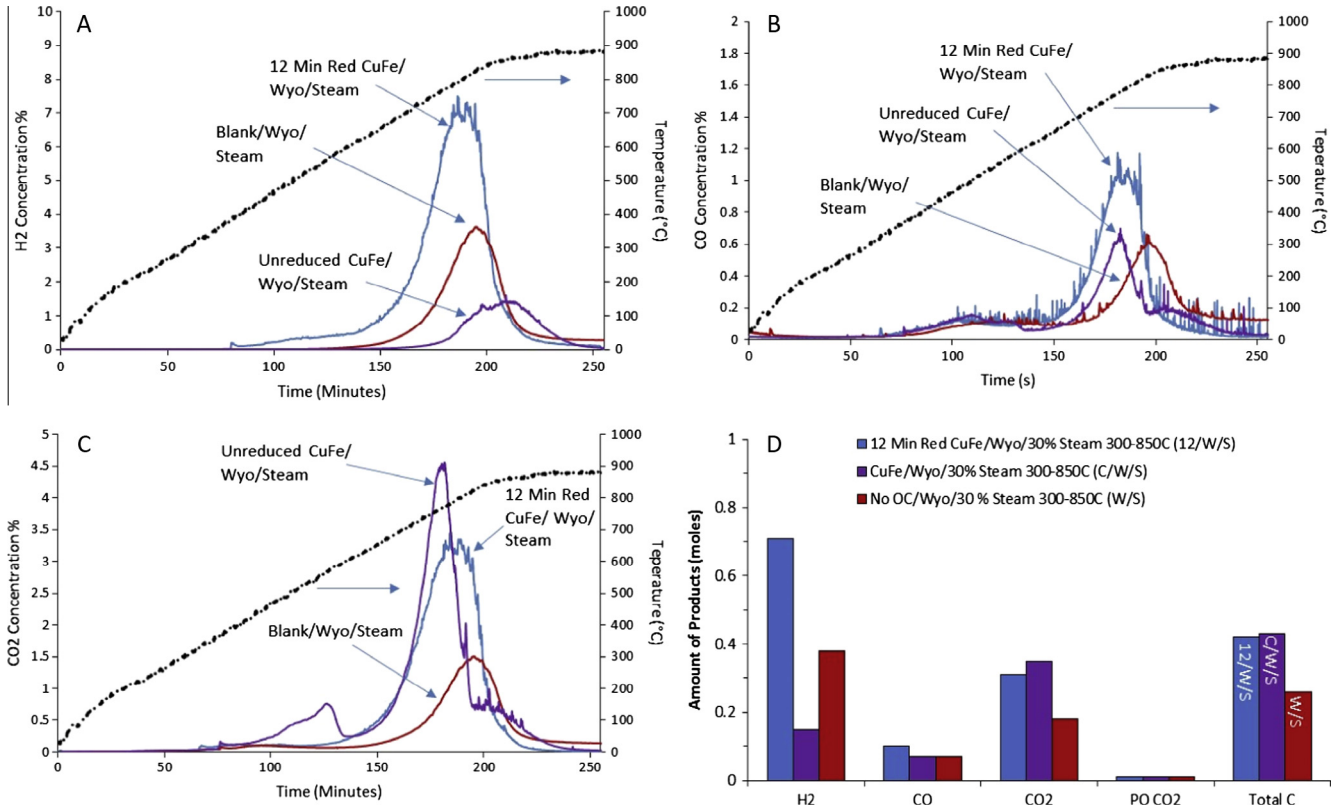

Fig. 8. Product gas composition during the temperature ramp (RT-850 °C) of reduced and unreduced copper ferrite oxygen carrier in the presence of 30% steam (300–850 °C) and Wyodak coal compared with the gasification of Wyodak coal in 30% Steam (300–850 °C) (A) H_2, (B) CO, (C) CO_2, (D) total molar production of gases.

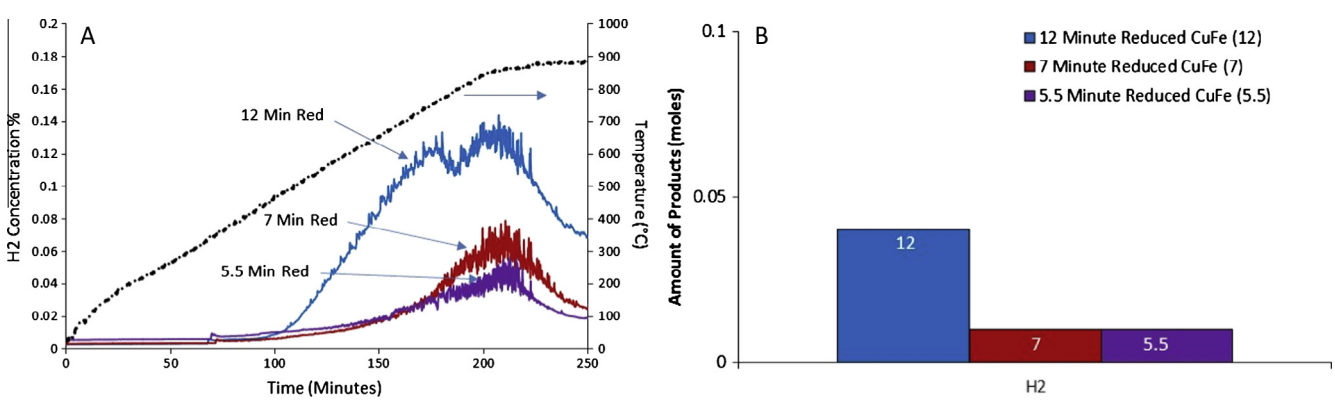

Fig. 9. Product gas composition during the temperature ramp (RT-850 °C) of reduced copper ferrite oxygen carrier in the presence of 30% steam (300–850 °C) (A) H_2, (B) total molar production.

and Illinois #6 coal/CuO-Fe_2O_3-alumina-with steam at 850 °C are shown in Fig. 11. When steam was introduced at 850 °C to Illinois #6 coal, the production of H_2 and CO was not complete after 90 min. When the oxygen carrier was present with coal/steam at 850 °C, both CO and CO_2 peak concentrations increased, indicating faster gasification of carbon and rapid reaction of CO to produce CO_2 in the presence of the oxygen carrier. During the temperature ramp of Illinois coal/CuO-Fe_2O_3-alumina without steam, the CO_2 peak was low, indicating minimal contribution from the CLOU reaction of CuO-Fe_2O_3 oxygen carrier with Illinois #6 coal, which was different from the observations with Wyodak coal. Oxygen released from the oxygen carrier was not able to react readily with Illinois #6, which is not a sub-bituminous coal like Wyodak coal. The differences in coal char properties of the two coals may have contributed to the differences in reactivities with oxygen. When steam was present during the temperature ramp, there was a significant increase in CO_2 and some increase in CO indicating that CuO-Fe_2O_3-alumina oxygen carrier promoted both carbon gasification and subsequent reaction to form CO_2.

The amounts of gases produced are also shown in Fig. 11. Total carbon produced during steam gasification at 850 °C was 0.37 mol, which is lower than (0.45 mol) when oxygen carrier was present, indicating that the oxygen carrier promoted more gasification of carbon. The CO_2 produced during the temperature ramp to 850 °C with oxygen carrier was about 0.17, moles which is possibly due to the oxygen release from CuO.

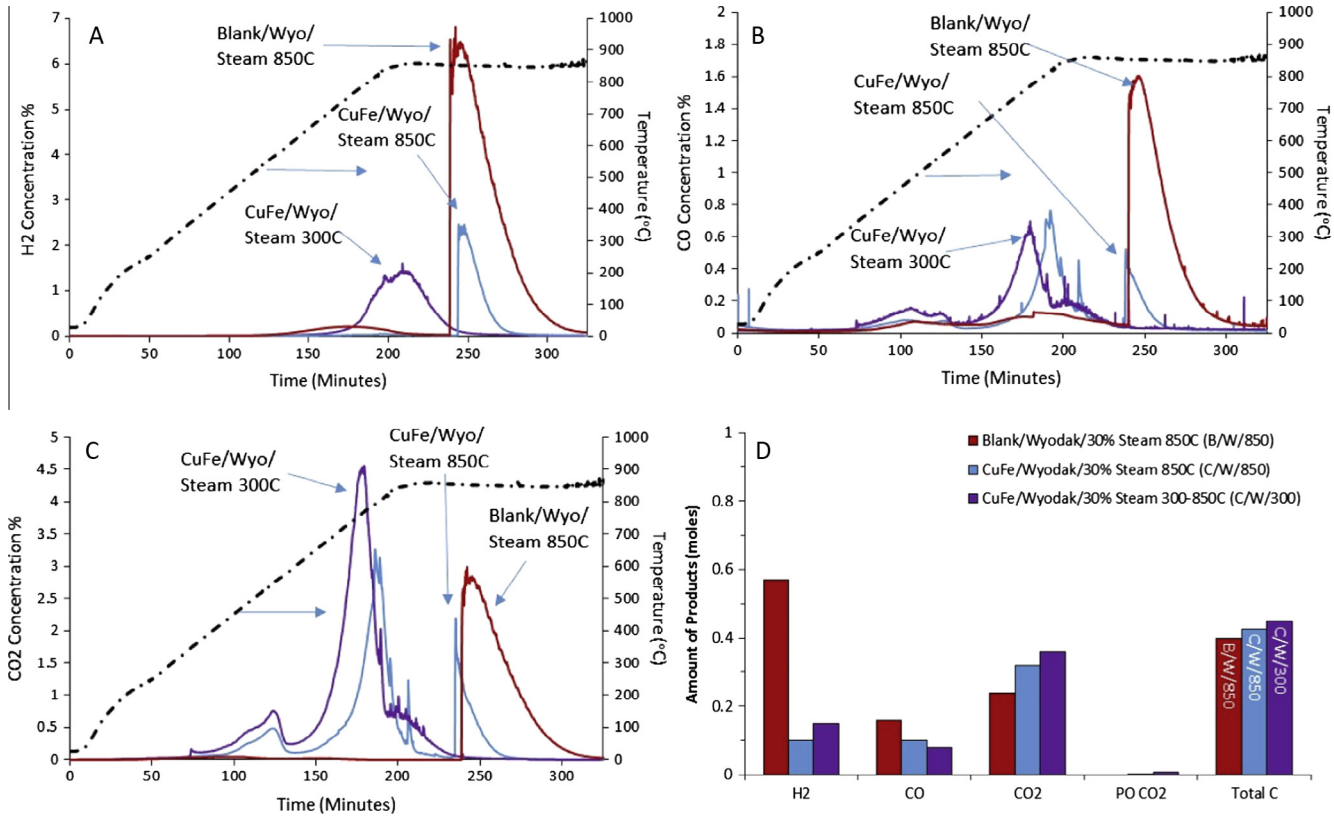

Fig. 10. Product gas composition during the temperature controlled reduction (RT-850 °C) of Wyodak coal with 30% steam addition at 850 °C with and without the copper ferrite oxygen carrier and Wyodak coal in the presence of the copper ferrite oxygen carrier and 30% steam (300–850 °C) (A) H_2, (B) CO, (C) CO_2, (D) total molar production of gases.

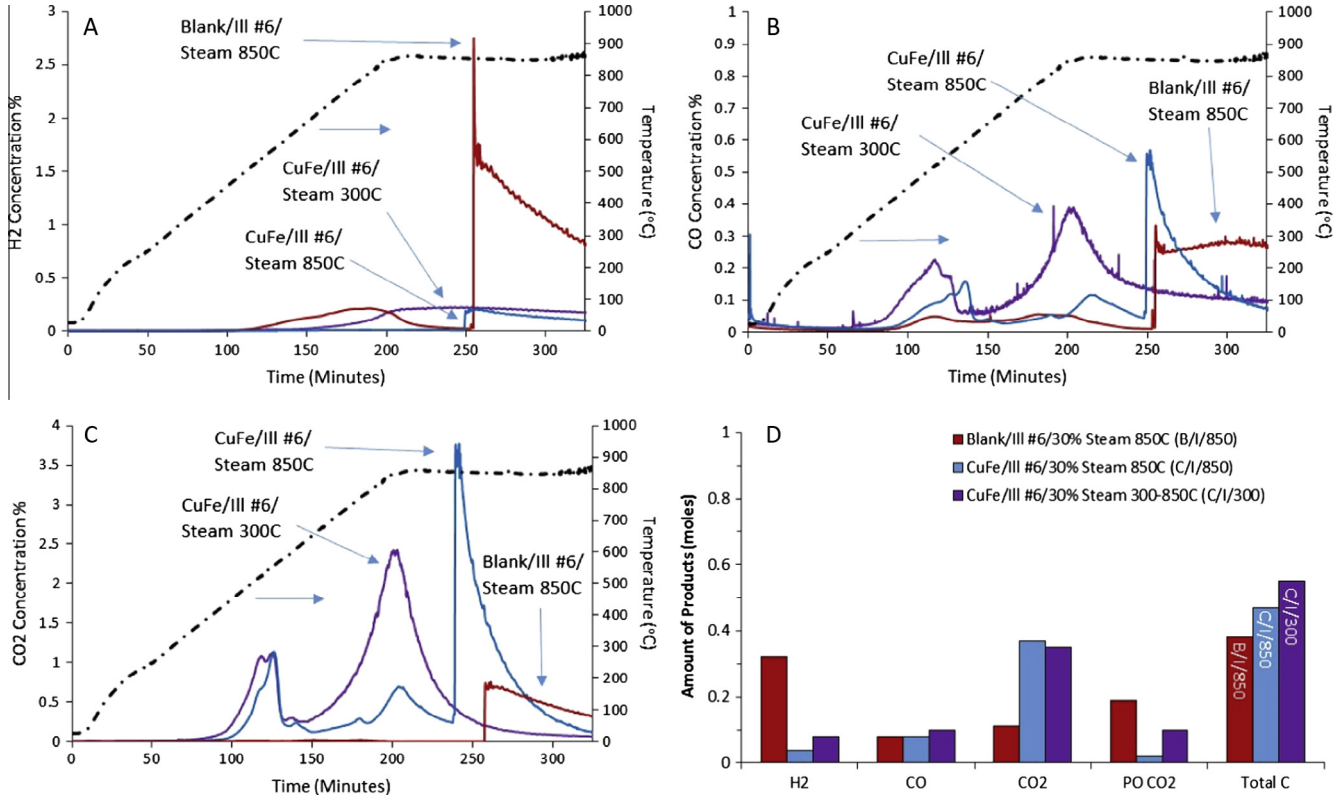

Fig. 11. Product gas composition during the temperature controlled reduction (RT-850 °C) of Illinois #6 coal with 30% steam addition at 850 °C with and without the copper ferrite oxygen carrier and Illinois #6 coal in the presence of the copper ferrite oxygen carrier and 30% steam (300–850 °C) (A) H_2, (B) CO, (C) CO_2, (D) total molar production of gases.

3.7. Diffuse reflectance infrared spectroscopic analysis (DRIFTS)

During the temperature ramp even without steam, the oxygen carrier reacted with coal to produce a substantial amount of CO_2. This production is more pronounced with Wyodak coal than with Illinois #6 coal. In addition to the reaction of gaseous oxygen produced by CLOU from the oxygen carrier, it is also possible that other volatile hydrocarbons were produced during the heating of the coals that reacted with either the oxygen carrier or the O_2 from CLOU. When the two coals were heated in a thermogravimetric analyzer (TGA) from ambient to 900 °C, in Argon weight losses (data not shown) were observed with both coals. The TGA weight loss from ambient to 500 °C with Illinois #6 coal and Wyodak coal were 25.72 wt.% and 37.88 wt.%, respectively. These weight losses may be due to coal devolatilization and are consistent with the data obtained during the fluidized test. During the TGA temperature ramp from 500 to 850 °C, weight loss with Illinois #6 was 11.48 wt.%, while it was 13.63 wt.% with

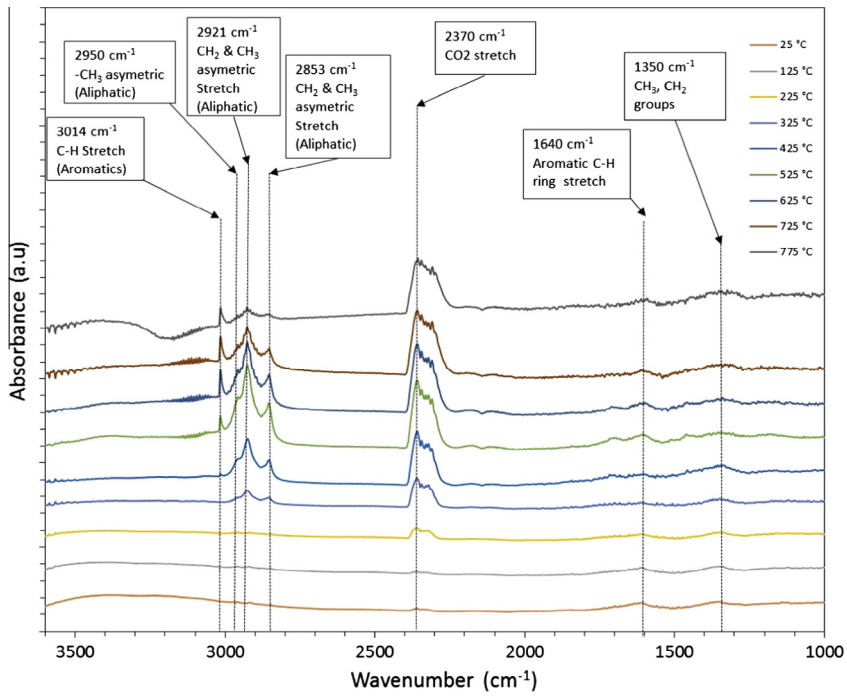

Fig. 12. Diffuse reflectance infrared Fourier transform spectroscopic (DRIFTS) data of Wyodak Coal during temperature ramp (Ambient-800 °C).

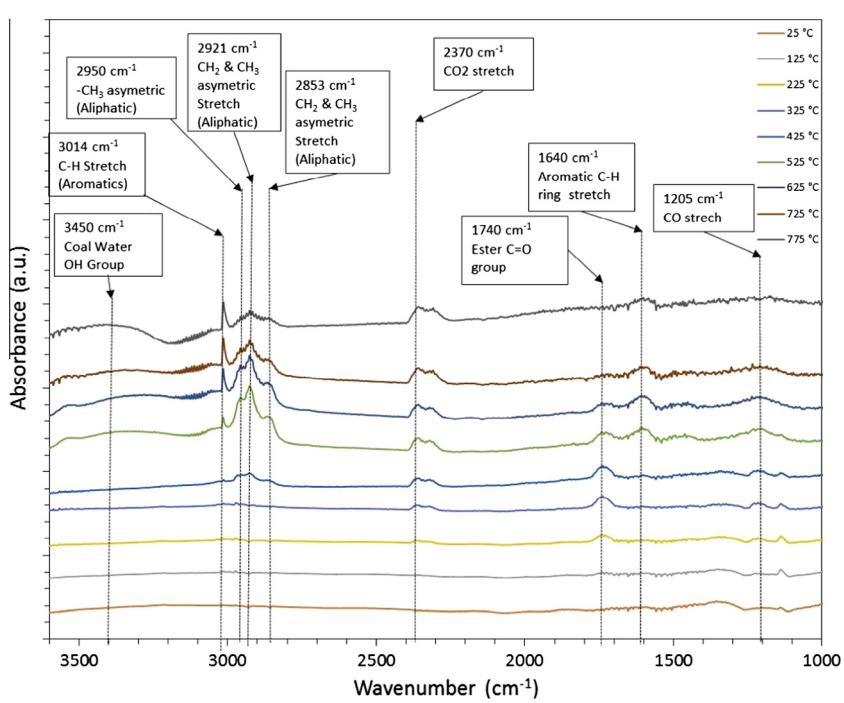

Fig. 13. Diffuse reflectance infrared Fourier transform spectroscopic (DRIFTS) data of Illinois #6 Coal during temperature ramp (Ambient-800 °C).

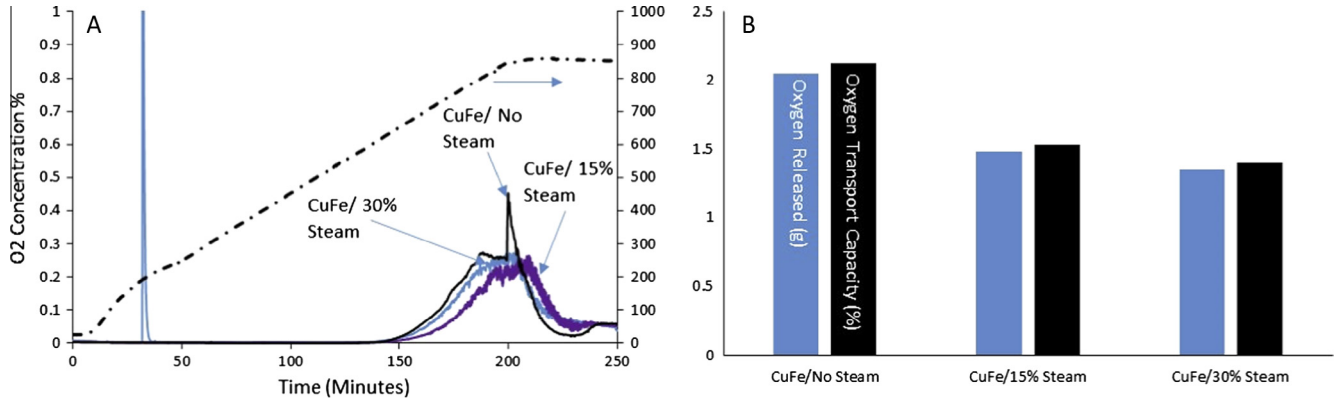

Fig. 14. Oxygen uncoupling product gas composition of the copper ferrite oxygen carrier during the temperature controlled reduction (RT-850 °C) with varying compositions of steam (300–850 °C) (A) O_2, (B) calculated oxygen transfer capacity.

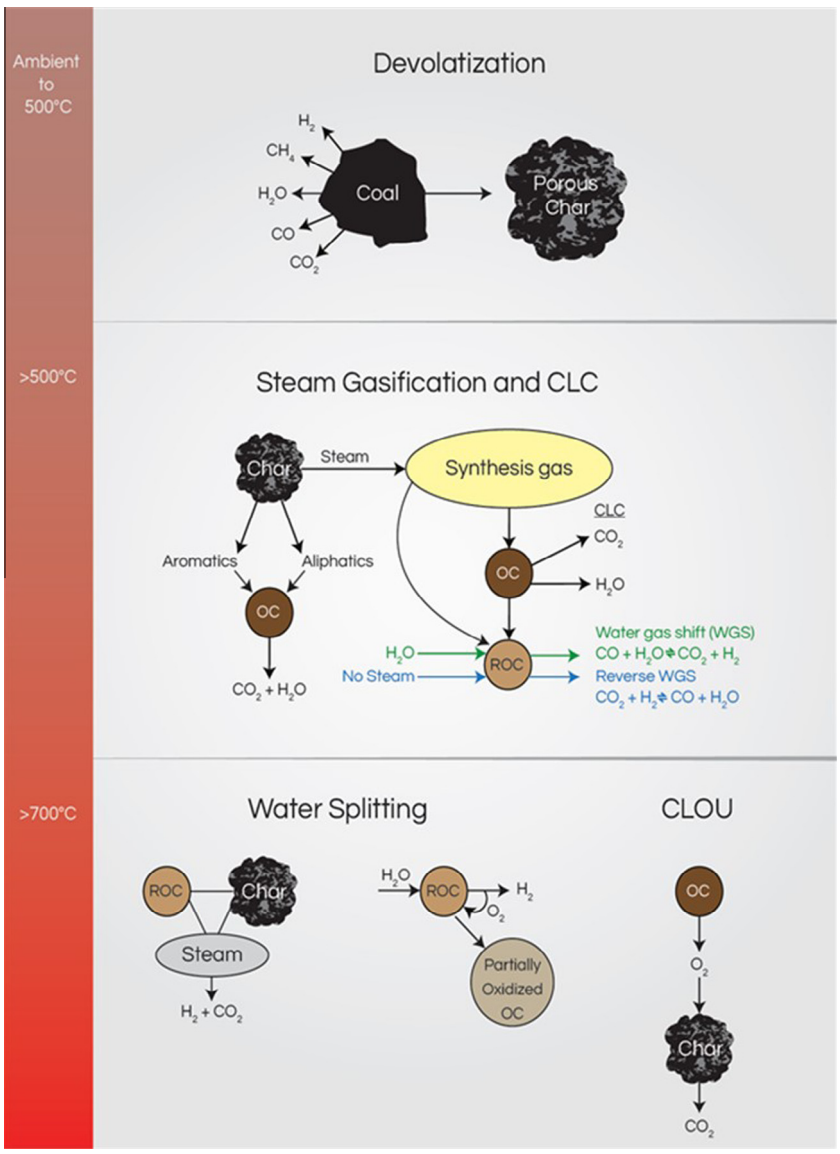

Fig. 15. Flow diagram of the contributing reactions in the coal/steam/oxygen carrier system.

Wyodak coal. Even though there was weight loss at 500–850 °C, H_2 and CO was not detected in this temperature range when coal was heated without steam during the temperature ramp in the fluidized bed.

Diffuse reflectance infrared spectroscopic (DRIFTS) analysis was conducted to understand the formation of these gaseous species/volatiles during the temperature ramp with both Wyodak and Illinois #6 coals. A Coal/quartz sample was placed in the DRIFTS

cell, and the system was flushed with helium to remove any residual air. Then the helium flow was terminated, and the sample was heated in helium remained in the cell while recording FTIR spectra at various temperatures.

The results with Wyodak coal at various temperatures are shown in Fig. 12. Peaks corresponding to aromatic C-H stretching at 2850, 2921 and 3014 cm^{-1} appeared around 325 °C and continued to grow when the temperature was increased to 625 °C. The data indicated that other volatile hydrocarbon species continued to form when the temperature was increased. The CO_2 peaks that were observed when Wyodak coal was heated with CuO-Fe-Al carrier may also be due to these hydrocarbons reacting with the oxygen carrier in addition to the reaction of oxygens directly with coal. However, it is difficult to quantify the hydrocarbon yields and the extent of the reactions with the oxygen carrier. Similar observations were observed with Illinois #6 coal as shown in Fig. 13.

3.8. Effect of steam on CLOU

In order to understand how the oxygen uncoupling reaction from the/CuO-Fe_2O_3-alumina oxygen carrier was affected by the presence of steam, a temperature ramp was conducted with CuO-Fe_2O_3-alumina oxygen carrier in the presence of 0%, 15% and 30% steam and the oxygen concentration from the effluent gas stream was analyzed during the temperature ramp.

As shown in Fig. 14, with increasing steam concentration, ion current corresponding to oxygen decreased, indicating a decrease in oxygen production with increasing steam concentration. The data indicated that presence of steam is not favorable for the oxygen uncoupling process, which is consistent with the data reported previously [59]. Steam has also been reported to be unfavorable for the reaction of synthesis gas with the oxygen carriers [60].

Based on the data reported in this paper, the reactions that occur during the temperature ramp with coal/CuO-Fe_2O_3-alumina oxygen carrier/steam are summarized in Fig. 15.

4. Conclusions

The steam gasification/combustion rates of both Wyodak and Illinois #6 coals were faster in the presence of the CuO-Fe_2O_3-alumina oxygen carrier. In addition to the increase in reaction rates, the total moles carbon oxides ($CO + CO_2$) formed from coal/steam were higher in the presence of the oxygen carrier. Gasification/combustion rates were faster with the sub-bituminous Wyodak coal than that with bituminous Illinois #6 coal. Reactions with simulated steam derived synthesis gas indicated that reduced oxygen carrier promoted the water-gas shift reaction when steam was present, while reverse water-gas shift reaction was promoted when steam was not present. The total amount of hydrogen production and rate of H_2 production increased when the partially reduced oxygen carrier reacted with coal/steam compared to either coal/steam or coal/steam/oxidised oxygen carrier. The main products with reduced oxygen carrier/coal/steam were H_2 and CO_2, which were different from the observations with un-reduced oxygen carrier. Water splitting reaction to produce H_2 was also observed with the reduced oxygen carrier. When steam was added at 850 °C, the coal gasification rates were faster than when steam was added at 300 °C. CuO-Fe_2O_3-alumina reacted with coal during the temperature ramp to 850 °C even in the absence of steam due to the CLOU reaction. CLOU reaction was found to be negatively affected by the increasing steam concentration. FTIR data indicated that volatile aromatic and aliphatic hydro carbons continued to increase during the temperature ramp from 325 to 625 °C.

Acknowledgements

This research was supported in part by an appointment to the National Energy Technology Laboratory Research Participation Program, sponsored by the U.S. Department of Energy and administered by the Oak Ridge Institute for science and education.

References

[1] Ishida M, Zheng D, Akehata T. Evaluation of a chemical-looping-combustion power-generation system by graphic exergy analysis. Energy 1987;12:147–54.
[2] Hatanaka T, Matsuda S, Hatano H. IECEC-97: proceedings of the thirty-second intersociety energy conversion engineering conference, vol. 1. Honolulu, Hawaii; 1997. p. 944–8.
[3] Richter HJ, Knoche KF. Reversibility of combustion process. ACS Symp Ser 1983;235:71–85.
[4] Ishida M, Jin H. A novel combustor based on chemical-looping reactions and its reaction kinetics. J Chem Eng Jpn 1994;27:296–301.
[5] Anheden M, Svedberg G. Exergy analysis of chemical looping combustion systems. Energy Convers Manage 1998;39:1967–80.
[6] Diego LF, Garcia-Labiano F, Adanez J, Gayan P, Abad A, Corbella BM, et al. Development of Cu-based oxygen carriers for chemical-looping combustion. Fuel 2004;83:1749–57.
[7] Garcia-Labiano F, Adanez J, Diego LF, Gayan P, Abad A. Effect of Pressure on the behavior of copper-, iron, and nickel-based oxygen carriers for chemical-looping combustion. Energy Fuels 2006;20:26–33.
[8] Gupta P, Velazquez-Vargas LG, Fan LS. Syngas redox (SGR) process to produce hydrogen from coal derived syngas. Energy Fuels 2007;21:2900–8.
[9] Kronberger B, Lyngfelt A, Loffler G, Hofbauer H. Design and fluid dynamic analysis of a bench-scale combustion system with CO_2 separation- chemical-looping combustion. Ind Chem Res 2005;44:546–56.
[10] M. Ishida, Jin H. Yokohma, United States Patent No. 5447,024, 2005. Bcbdgf.
[11] Shen L, Wu J, Xiao J, Song Q, Xiao R. Chemical looping combustion of biomass in a 10 kWth reactor with iron oxide as an oxygen carrier. Energy Fuels 2009;23:2498–505.
[12] Siriwardane R, Tian H, Richards G, Simonyi T, Poston J. Chemical-looping combustion of coal with metal oxide oxygen carriers. Energy Fuels 2009;23:3885–92.
[13] Cao Y, Casenas B, Pan W. Investigation of chemical looping combustion of solid fuels. Energy Fuels 2006;20:1845–54.
[14] Lyon RK, Cole JA. Unmixed combustion: an alternative to fire. Combust Flame 2000;121:249–61.
[15] Scott SA, Dennis JS, HayHurst AN, Brown T. *In situ* gasification of a solid fuel and CO_2 Separation using chemical looping. Am Inst Chem Eng 2006;52:3325–8.
[16] Lyngfelt A, Johansson M, Mattisson T. Chemical looping combustion status and development. 9th International conference on circulating fluidized beds, Hamburg, Germany, May 13–16, 2008.
[17] Adanez J, Abad A, Garcia-Labiano F, Gayan P, Diego L. Progress in chemicals-looping combustion and reforming technologies. Prog Energy Combust Sci 2012;38:215–82.
[18] Lyngfelt A. Chemical looping combustion of solid fuels – status and development. Appl Energy 2014;113:1869–73.
[19] Fan LS. Chemical looping systems for fossil energy conversions. John Wiley and Sons Inc.; 2010.
[20] Anthony EJ. Solid looping cycles: a new technology for coal conversion. Ind Eng Chem Res 2008;47:1747–54.
[21] Henderson C. Chemical looping combustion of coal. IEA Clean Coal Center; 2010.
[22] Ge H, Shen L, Gu H, Jiang S. Effect of co-precipitation and impregnation on K-decorated Fe_2O_3/Al_2O_3 oxygen carrier in chemical looping combustion of bituminous coal. Chem Eng J 2015;262:1065–76.
[23] Arjmand M, Leion H, Mattisson T, Lyngfelt A. Investigation of different manganese ores as oxygen carriers in chemical-looping combustion (CLC) for solid fuels. Appl Energy 2014;113:1883–94.
[24] Mendiara T, Diego L, García-Labiano F, Gayán P, Abad A, Adánez J. On the use of a highly reactive iron ore in chemical looping combustion of different coals. Fuel 2014;126:239–49.
[25] Saucedo M, Lim J, Dennis J, Scott S. CO_2-gasification of a lignite coal in the presence of an iron-based oxygen carrier for chemical-looping combustion. Fuel 2014;127:186–201.
[26] Yang W, Zhao H, Ma J, Mei D, Zheng C. Copper-decorated hematite as an oxygen carrier for in situ gasification chemical looping combustion of coal. Energy Fuels Energy Fuels 2014;28:3970–81.
[27] Fan Y, Siriwardane R. Novel new oxygen carriers for chemical looping combustion of solid fuels. Energy Fuels Energy Fuels 2014;28:2248–57.
[28] Abad A, Adánez J, Gayán P, Diego L, García-Labiano F, Sprachmann G. Conceptual design of a 100 MWth CLC unit for solid fuel combustion. Appl Energy 2015;157:462–74.
[29] Abad A, Pérez-Vega R, Diego L, García-Labiano F, Gayán P, Adánez J. Design and operation of a 50 kWth chemical looping combustion (CLC) unit for solid fuels. Appl Energy 2015;157:295–303.
[30] Bayham S, McGiveron O, Tong A, Chung E, Kathe M, Wang D, et al. Parametric and dynamic studies of an iron-based 25-kWth coal direct chemical looping unit using sub-bituminous coal. Appl Energy 2015;145:354–63.

[31] Lyngfelt A, Leckner B. A 1000 MWth boiler for chemical-looping combustion of solid fuels – discussion of design and costs. Appl Energy 2015;154:475–87.
[32] Ma J, Zhao H, Tian X, Wei Y, Rajendran S, Zhang Y, et al. Chemical looping combustion of coal in a 5 kWth interconnected fluidized bed reactor using hematite as oxygen carrier. Appl Energy 2015;157:304–13.
[33] Ohlemüller P, Alobaid F, Gunnarsson A, Ströhle J, Epple B. Development of a process model for coal chemical looping combustion and validation against 100 kWth tests. Appl Energy 2015;157:433–48.
[34] Ströhle J, Orth M, Epple B. Chemical looping combustion of hard coal in a 1 MWth pilot plant using ilmenite as oxygen carrier. Appl Energy 2015;157:288–94.
[35] Adánez J, Abad A, Perez-Vega R, Diego L, García-Labiano F, Gayán P. Design and operation of a coal-fired 50 kWth chemical looping combustor. Energy Proc 2014;63:63–72.
[36] Linderholm C, Knutsson P, Schmitz M, Markström P, Lyngfelt A. Material balances of carbon, sulfur, nitrogen and ilmenite in a 100 kW CLC reactor system. Int J Greenhouse Gas Control 2014;27:188–202.
[37] Luo S, Bayham S, Zeng L, Mcgiveron O, Chung E, Majumder A, et al. Conversion of metallurgical coke and coal using a coal direct chemical looping (CDCL) moving bed reactor. Appl Energy 2014;118:300–8.
[38] Markström P, Linderholm C, Lyngfelt A. Operation of a 100 kW chemical-looping combustor with Mexican petroleum coke and Cerrejón coal. Appl Energy 2014;113:1830–5.
[39] Ströhle J, Orth M, Epple B. Design and operation of a 1 MWth chemical looping plant. Appl Energy 2014;113:1490–5.
[40] Thon A, Kramp M, Hartge E, Heinrich S, Werther J. Operational experience with a system of coupled fluidized beds for chemical looping combustion of solid fuels using ilmenite as oxygen carrier. Appl Energy 2014;118:309–17.
[41] Tong A, Bayham S, Kathe M, Zeng L, Luo S, Fan L. Iron-based syngas chemical looping process and coal-direct chemical looping process development at Ohio State University. Appl Energy 2014;113:1836–45.
[42] Mattison T, Lyngfelt A, Leion L. Chemical looping with oxygen uncoupling for combustion of solid fuels. Int J Greenhouse Gas Control 2009;3:11–9.
[43] Coppola A, Solimene R, Bareschino P, Salatino P. Mathematical modeling of a two-stage fuel reactor for chemical looping combustion with oxygen uncoupling of solid fuels. Appl Energy 2015;157:449–61.
[44] Dansie J, Sahir A, Hamilton M, Lighty J. An investigation of steam production in chemical-looping combustion (CLC) and chemical-looping with oxygen uncoupling (CLOU) for solid fuels. Chem Eng Res Des 2015;94:12–7.
[45] Peltola P, Ritvanen J, Tynjälä T, Hyppänen T. Fuel reactor modelling in chemical looping with oxygen uncoupling process. Fuel 2015;147:184–94.
[46] Sahir A, Dansie J, Cadore A, Lighty J. A comparative process study of chemical-looping combustion (CLC) and chemical-looping with oxygen uncoupling (CLOU) for solid fuels. Int J Greenhouse Gas Control 2014;22:237–43.
[47] Adánez-Rubio I, Arjmand M, Leion H, Gayán P, Abad A, Mattisson T, et al. Investigation of combined supports for Cu-based oxygen carriers for chemical looping with oxygen uncoupling (CLOU). Energy Fuels 2013;27:3918–27.
[48] Siriwardane R, Tian H, Miller D, Richards G, Simonyi T, Poston J. Evaluation of reaction mechanism of coal–metal oxide interactions in chemical-looping combustion. Combust Flame 2010;157:2198–208.
[49] Siriwardane R, Ksepko E, Tian T, Poston J, Simonyi T, Sciazko M. Interaction of iron–copper mixed metal oxide oxygen carriers with simulated synthesis gas derived from steam gasification of coal. Appl Energy 2013;107:111–23.
[50] Siriwardane R, Tian H, Simonyi T, Poston J. Synergetic effects of mixed copper–iron oxides oxygen carriers in chemical looping combustion. Fuel 2013;108:319–33.
[51] Monazam ER, Breault RW, Tian H, Siriwardane R. Reaction kinetics of mixed $CuO-Fe_2O_3$ with methane as oxygen carriers for chemical looping combustion. Ind Eng Chem Res 2015;54:11966–74.
[52] Siriwardane S, Tian H, Miller D, Richards G. Fluidized bed testing of commercially prepared MgO-promoted hematite and $CuO–Fe_2O_3$ mixed metal oxide oxygen carriers for methane and coal chemical looping combustion. Appl Energy 2015;157:348–57.
[53] Siriwardane R, Tian H, Fisher J. Production of pure hydrogen and synthesis gas with Cu-Fe oxygen carriers using combined processes of chemical looping combustion and methane decomposition/reforming. Int J Hydrogen Energy 2015;40:1698–708. Gasification faster in the presence of OC.
[54] Leon H, Jerndal E, Steenari BM, Hermansson S, Israelsson M, Jansson E, et al. Solid fuels in chemical looping combustion using oxide scale and unprocessed iron ore as oxygen carriers. Fuel 2009;88:1945–54.
[55] Bao J, Li Z, Cai N. Experiments of char particle segregation effect on the gas conversion behavior in the fuel reactor for chemical looping combustion. Appl Energy 2014;113:1874–82.
[56] Chen L, Liu F, Heather SN, Fan Z, Liu K. Coal char-fueled chemical looping combustion use different iron- based oxygen carriers. Energy Proc 2014;63:5172–7.
[57] Kulaots I, Hsu A, Suuberg EM. The role of porosity in char combustion. Proc Combust Inst 2007;31:1897–903.
[58] Zygourakis K. The effects of pyrolysis conditions on the macropore structure of coal chars. Prepr Pap- Am Chem Soc, Div Fuel Chem 1988;33:951–9.
[59] Zhang Y, Liu F, Chen L, Han C, Richurg LR, Neathery JK, et al. Investigation of the water vapor influence on the performance of iron-, copper-, and nickel-based oxygen carriers for chemical looping combustion. Energy Fuels 2013;27:5341–51.
[60] Rubel AM, Zhang Y, Neathery JK, Lui K. Effect of water vapor on the redox reactions of iron based oxygen carriers for chemical looping combustion. Energy Fuels 2011;25:4271–9.